Journal of Superconductivity, Vol. 7, No. 2, 1994

Investigation of the Temperature Dependence of Electron and Phonon Raman Scattering in Single Crystal $YBa_2Cu_3O_{6.952}$

G. Blumberg,[1,2] M. V. Klein,[1] L. Börjesson,[3] R. Liang,[4] and W. N. Hardy[4]

Received 31 July 1993

Detailed Raman-scattering measurements have been performed on high-quality $YBa_2Cu_3O_{6.952}$ single crystal ($T_c = 93$ K, $\Delta T_c = 0.3$ K). A sharp (FWHM 7.2 cm^{-1} at 70 K and 10.0 cm^{-1} at 110 K) 340 cm^{-1} phonon mode has been observed in B_{1g} polarization. An electronic scattering peak at 500 cm^{-1} in the B_{1g} polarization extends down to 250 cm^{-1}. These FWHM values determine the upper limit of the homogeneous linewidth of the phonon and electronic excitations. The start of the electronic spectral function renormalization and of the 340 cm^{-1} mode anomalies (frequency softening, linewidth sharpening, and intensity increase) have been observed to occur approximately 40 K above T_c. The 340 cm^{-1} mode Fano shape analysis has been performed and the temperature dependences of the Fano shape parameters have been estimated. All 340 cm^{-1} mode anomalies have been explained by the electronic spectral function renormalization.

KEY WORDS: Raman scattering; electron–phonon coupling.

1. INTRODUCTION

One of the unusual characteristics of the high-temperature superconductors is the strong background in Raman scattering in a very broad frequency range [1–5]. At the low temperatures the low-frequency part of the background renormalizes, and the lowest frequency intensity redistributes into a broad peak at around 300–500 cm^{-1} depending on scattering symmetry [6,7]. The background is thought to be of electronic origin and the general view of the redistribution of intensity below T_c is that it is related to the opening of a superconducting gap, the peak being the characteristic pair breaking energy. However, even for the lowest temperatures measured, a linearly increasing intensity contribution has been observed below the "gap" value.

In $YBa_2Cu_3O_{7-\delta}$ the electronic spectral function renormalization at the low temperatures affects the 340 cm^{-1} O(2), O(3) oxygen out-of-phase vibrational mode. The line-shape of this mode is strongly asymmetric and shows typical Fano interference effects [8,9] which indicate an interaction with the electronic continuum scattering. Further strong evidence for the interaction of the mode with electronic states is provided by anomalies in the temperature dependences of the frequency, halfwidth, and intensity that occur around T_c. It was earlier observed by Raman scattering that the frequency of the mode softens remarkably below T_c [10]. The softening around T_c has recently also been observed by inelastic neutron scattering for momentum transfers throughout the Brillouin zone [11]. Furthermore, the Raman intensity of the 340 cm^{-1} mode increases below T_c [12,5]. However, the temperature dependence of the linewidth displays different behavior around T_c, ranging from sharpening to broadening, depending on the crystal growing condition and oxygen content [13,14]. The self-energy effects on the frequency and the line-width of the

[1]Department of Physics, Materials Research Laboratory and Science and Technology Center for Superconductivity, University of Illinois at Urbana-Champaign, Urbana, Illinois 61801-3080.
[2]Institute of Chemical Physics and Biophysics, Rävala 10, Tallinn EE0001, Estonia.
[3]Department of Physics, Chalmers University of Technology S-41296 Gothenburg, Sweden.
[4]Physics Department, University of British Columbia Vancouver, B.C. V6T 1Z1 Canada.

0896-1107/94/0400-0445$07.00/0

340 cm^{-1} mode have been used for determinations of the superconducting gap [14–16] using strong coupling models [17,18].

In this paper we report on a detailed investigation of the low-frequency behavior of the electronic Raman background as a function of temperature and its interaction with the 340 cm^{-1} O(2), O(3) phonon of B_{1g} symmetry.

2. EXPERIMENTAL

The Raman experiments were carried out on a $YBa_2Cu_3O_{6.952}$ single crystal characterized in [19]. The crystal shows a sharp superconducting transition at $T_c = 93$ K ($\Delta T_c = 0.3$ K). The crystal was mounted on a cold finger of a liquid-helium cryostat (CryoVac). Laser light from an Ar^+ laser with a wavelength of 4880 Å and power of 300 μW was focused by microscope optics (Nikon M plan 100×/NA= 0.75 SLWD) to a spot with a diameter of 5 μm. The same microscope optics was used for the collection of the scattered light in a strict backscattering geometry. The collected scattered light was analyzed by a triple grating spectrometer (SPEX 1877) with CCD detector (Wright Instruments AT1). In one set of spectra a stop was mounted in the middle of the second slit, i.e., the slit in between the two gratings of the filter stage, to be able to measure simultaneously the Stokes and anti-Stokes spectrum from −500 to +800 cm^{-1}. The Stokes and anti-Stokes spectra enabled us to determine the actual temperature within the laser spot by considering the thermal occupation factor. The laser illumination was found to cause a heating of about 50 K. All spectra were corrected for the Bose factor with the corrected temperature.

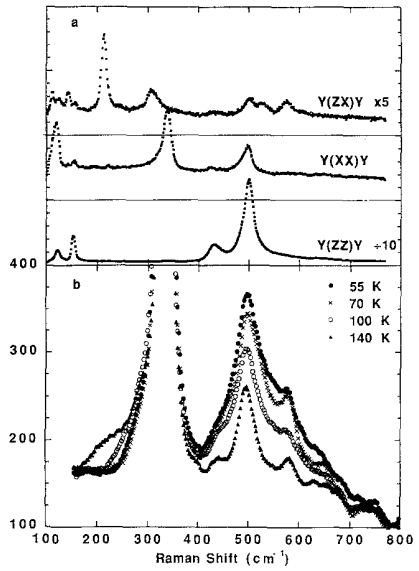

Fig. 1. (a) Room-temperature Raman spectra for $y(zx)y$, $y(xx)y$, and $y(zz)y$ scattering geometries. The spectra correspond to $B_{2g}+B_{3g}$, $A_{1g}+B_{1g}$, and A_{1g} symmetries, respectively. The instrumental resolution (FWHM) is 10 cm^{-1}. (b) The low-intensity part of the Raman spectra for $z(x'y')z$ scattering geometry above and below T_c. Spectra are corrected for the Bose population factor by subtracting the anti-Stokes spectrum from the Stokes spectrum. The narrow peak at 500 cm^{-1} is the O(4) A_{1g} mode observed in this symmetry due to the orthorhombic distortion. The instrumental resolution (FWHM) is 19 cm^{-1}.

3. RESULTS

3.1. Room-Temperature Spectral in Different Symmetries

In Fig. 1a we present the room temperature spectra in $y(zx)y$, $y(xx)y$ and $y(zz)y$ scattering geometries. In Table I we summarize the frequencies of the different modes, their symmetry and assignments, together with a comparison with the data on a twin-free single crystal [20]. All oxygen modes including B_{2g} and B_{3g} vibrations show asymmetric Fano shape, which is evidence of fairly strong oxygen phonon interactions with the electronic continuum in all symmetries, including $B_{2g}+B_{3g}$ symmetry. Except for a very weak line at around 222 cm^{-1} in the $x(zz)x$ and $y(xx)y$ polarization (about 200 times lower intensity than the 500 cm^{-1} mode) and some weak intensity at 125 cm^{-1} in the $y(zx)y$ polarization, the crystal does not show any extra features intrinsic to impurities, defects, vacancies, or oxygen disorder. This proves the high quality of the crystal.

3.2. Anomalies Around T_c for the 340 cm^{-1} Mode

In Fig. 2a we show spectra in the frequency range around the 340 cm^{-1} mode recorded at temperatures between 70 and 200 K. The spectra display the asymmetric line shape that has been reported before and is thought to arise from Fano-type interference effects between the phonon and the flat electronic continuum scattering. As seen from Fig. 2, the 340 cm^{-1} mode frequency starts to soften at temperatures below 140 K. Furthermore, the intensity starts to increase below the same temperature. A small sharpening of the line is also noted below 140 K. These phonon anomalies start at about 40 K about T_c in the same

Table I. Raman Phonon Frequencies as Observed in Different Polarization Geometries with the Incident and Scattered Light along the *a*- or *b*-axis and Comparison with the Data [20] (in brackets), Their Symmetries, and the Normal Mode Assignment

Scattering geometry				
$x(zz)x+y(zz)y$	$y(xx)y+x(yy)x$	$y(zx)y+x(zy)x$	Symmetry	Assignment
122.5(119+119)[a]	119(119+115)	112	A_g	Ba_z
		125		
		142.5(142+140)	B_{2g}, B_{3g}	$Cu(2)_{x+y}$
153(149+149)	154	156	A_g	$Cu(2)_z$
		212(210+···)	B_{2g}	$O(4)_x$
224 vw	221.5 vw			
		306(···+303)	B_{3g}	$O(4)_y$
339.5 vw	337.5(336+336)		A_g	$O(2), O(3)_z$
431(435+435)	425 vw	431 vw	A_g	$O(2), O(3)_z$
500(497+498)	497(···+495)	502.5	A_g	$O(4)_z$
		525(···+526)	B_{3g}	$O(2), O(3)_y$
		574(579+···)	B_{2g}	$O(2), O(3)_x$

[a]All values in cm^{-1}.

region where Liang *et al.* observed a downward deviation from linearity in the resistivity temperature dependence [19]. These phonon anomalies above T_c are in contrast to previous studies, where the anomalies have been observed to occur at approximately T_c, at least for pure $YBa_2Cu_3O_7$ [21]; however, as observed by Raman and IR measurements [22,23], a pronounced frequency softening for both $YBa_2Cu_4O_8$ and $Y_2Ba_4Cu_7O_{15}$ was found to start well above T_c.

In Fig. 2b we present some spectra from Fig. 2a deconvoluted with the instrumental resolution profile by a Fourier-transformation method. We obtained a FWHM of 7.2 cm^{-1} at 70 K and 10.0 cm^{-1} at 110 K. The typical FWHM observed in the previous works was larger than 13 cm^{-1} [13], and the sharpest Fano line shapes, 11 cm^{-1} for the $YBa_2Cu_3O_{6.952}$ sample and 10 cm^{-1} for the $YBa_2Cu_3O_{6.9}$ sample at the lowest measured temperature, have been observed in the recent work [14]. The 340 cm^{-1} mode broadening could be due to inhomogeneity, and the sharpest observed modes give an estimation of the upper limit of the homogeneous linewidth.

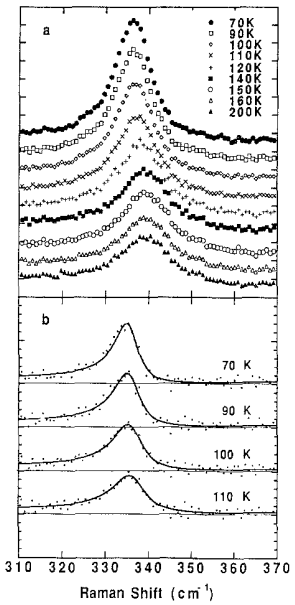

Fig. 2. (a) Temperature dependence of the B_{1g} O(2), O(3) out-of-phase vibration. Note the decreasing peak frequency and increasing intensity for temperatures below 120 K. The instrumental resolution (FWHM) is 5.5 cm^{-1}. (b) The Raman spectra above deconvoluted with the instrumental resolution profile. The zero level is indicated with a horizontal line for each spectrum. The solid curves are calculated from Eq. (1) with parameters described in the text.

3.3. Redistribution of the Electronic Density of States

In Fig. 1b we present the electronic density redistribution around the superconducting transition in $z(x'y')z$ polarization. Apart from the 340 cm^{-1} mode of B_{1g} symmetry and the 500 cm^{-1} mode that is observed in $z(x'y')z$ polarization due to the slight orthorhombic distortion, Fig. 1b displays clear features of electronic scattering intensity reduction below the 340 cm^{-1} mode and the appearance of a broad peak under the 500 cm^{-1} phonon mode. All changes again start about 40 K above T_c, and develop between 140 and 70 K; further temperature decrease does not result in appreciable changes in the electronic scattering redistribution. Below T_c the broad

500 cm^{-1} peak shape does not extend below 250 cm^{-1}, but some unstructured low-frequency Raman intensity remains even at lowest temperatures.

4. THE 340 cm^{-1} MODE FANO SHAPE ANALYSIS

In order to describe the temperature dependence of the 340 cm^{-1} mode we fitted all Fano shapes below 130 K as presented in Fig. 2. These fittings were obtained with the expression

$$I(E) = T_e^2[\pi\rho(E)(\omega_0 - E - \nu T_{ph}/T_e)^2 + \gamma(\nu R(E) - T_{ph}/T_e)^2 + \pi\rho(E)\gamma(\nu^2\pi\rho(E) + \gamma)]/[(\omega_0 - E + \nu^2 R(E))^2 + (\nu^2\pi\rho(E) + \gamma)^2] \quad (1)$$

where ω_0 and γ are the bare phonon self-energy and the HWHM, $-R(E) + i\pi\rho(E)$ is the electronic Green's function, T_{ph} and T_e are the phonon and the electronic continuum transition matrix elements, and ν is the electron phonon interaction constant [24]. For the simplest approach we used $\rho(E) \sim \Gamma_{2\Delta}/((2\Delta - E)^2 + \Gamma_{2\Delta}^2)$, which describes reliably the broad electronic peak around 510 cm^{-1}. As output to the fits, we obtained the bare phonon self-energy $\omega_0 =$ 337 cm^{-1}, the transition matrix elements ratio $T_{ph}/T_e = 0.314$, the electron–phonon interaction constant $\nu = 25$ cm^{-1}, and for $\rho(E)$ function the value $2\Delta =$ 510 cm^{-1}. Only $\gamma(T)$ and $\Gamma_{2\Delta}(T)$ were used as temperature-dependent fitting parameters. For $2\gamma(T)$ we obtained a continuous decrease with temperature from 11.5 cm^{-1} at 160 K to 3 cm^{-1} at 70 K. This does not show any bare phonon anomalies around T_c. For $2\Gamma_{2\Delta}(T)$ we obtained sharpening from 850 cm^{-1} at 110 K when the electronic scattering peak acquires noticeable intensity to 500 cm^{-1} at 70 K. Some fit results are presented in Fig. 2b by the solid line. The simplest approach describes quite well all the observed temperature dependence anomalies of the 340 cm^{-1} phonon: softening, sharpening, and intensity increase. We note that for satisfactory fitting we do not need any additional noninteracting background parameters or functions such as those that have been used in a number of previous works [21].

This work was supported by Swedish Natural Sciences Research Council (G.B. and L.B.) and by the National Science Foundation (DMR 91-20000) through the Science and Technology Center for Superconductivity (G.B. and M.V.K.).

REFERENCES

1. S. Sugai, Y. Entomoto, and T. Murakami, *Solid State Commun.* **72**, 1193 (1989).
2. D. Reznik, A. L. Kotz, S. L. Cooper, M. V. Klein, W. C. Lee and D. M. Ginsberg, in *Proceedings of the International Workshop on Electronic Properties and Mechanisms of High-T_c Superconductivity (IWEPM), Tsukuba, Japan, 1991*, T. Ocuchi, K. Kadowaki, and T. Sasaki, eds. (North-Holland, Amsterdam, 1992), pp. 283–287.
3. S. L. Cooper, D. Reznik, P. Nyhus, M. V. Klein, W. C. Lee, D. M. Ginsberg, B. W. Veal, A. P. Paulikas, and B. Dabrowski, *Phys. Rev. Lett.* **70**, 1533 (1993).
4. A. A. Maksimov, A. V. Puchkov, I. I. Tartakovskii, D. Reznik, M. V. Klein, W. C. Lee, and D. M. Ginsberg, *Sov. Phys. JETP* **56**, 570 (1992).
5. D. Reznik, S. L. Cooper, M. V. Klein, W. C. Lee, D. M. Ginsberg, A. A. Maksimov, A. V. Puchkov, I. I. Tartakovskii, and S.-W. Cheong, *Phys. Rev. B* **48**, 7624 (1993).
6. S. L. Cooper, M. V. Klein, B. G. Pazol, J. P. Rice, and D. M. Ginsberg, *Phys. Rev. B* **37**, 5920 (1988).
7. R. Hackel, W. Gläser, P. Müller, D. Einzel, and K. Andres, *Phys. Rev. B* **37**, 7133 (1988).
8. S. L. Cooper, F. Slakey, M. V. Klein, J. P. Rice, E. D. Bukowski, and D. M. Ginsberg, *Phys. Rev. B* **38**, 11934 (1988).
9. C. Thomsen, M. Cardona, B. Gegenheimer, R. Liu, and A. Simon, *Phys. Rev. B* **37**, 9860 (1988).
10. R. M. Macfarlane, H. J. Rosen, and H. Seki, *Solid State Commun.* **63**, 831 (1987).
11. N. Pyka, W. Reichardt, L. Pintschovius, G. Engel, J. Rossat-Mignod, and J. Y. Henry, *Phys. Rev. Lett.* **70**, 1457 (1993).
12. B. Friedl, C. Thomsen, H.-U. Habermeier, and M. Cardona, *Solid State Commun.* **78**, 291 (1991).
13. See, for example, C. Thomsen and M. Cardona, *Physica C* **206**, 137 (1993), and references therein.
14. E. Altendorf, X. K. Chen, J. C. Irwin, R. Liang, and W. N. Hardy, *Phys. Rev. B.* **47**, 8140 (1993).
15. C. Thomsen, M. Cardona, B. Friedl, C. O. Rodriguez, I. I. Mazin, and O. K. Andersen, *Solid State Commun.* **75**, 219 (1990).
16. B. Friedl, C. Thomsen, and M. Cardona, *Phys. Rev. Lett.* **65**, 915 (1990).
17. R. Zeyher and G. Zwicknagl, *Z. Phys. B, Condensed Matter* **78**, 175 (1990).
18. F. Marsiglio, R. Akis, and J. P. Carbotte, *Phys. Rev. B* **45**, 9865 (1992).
19. R. Liang, P. Dosanjh, D. A. Bonn, D. J. Baar, J. F. Carolan, and W. N. Hardy, *Physica C* **195**, 51 (1992).
20. K. F. McCarty, J. Z. Liu, R. N. Shelton, and H. B. Radousky, *Phys. Rev. B.* **41**, 8792 (1990).
21. See, for example, C. Thomsen, in *Light Scattering in Solids VI*, M. Cardona, ed., Topics in Applied Physics, Vol. 68 (Springer, Berlin, Heidelberg 1991), p. 285 and references therein.
22. A. P. Litvinchuk, C. Thomsen, and M. Cardona, *Solid State Commun.* **83**, 343 (1992).
23. A. P. Litvinchuk, C. Thomsen, M. Cardona, J. Karpinski, E. Kaldis, and S. Rusiecki, preprint.
24. G. Blumberg, L. Börjesson, R. Liang, and W. N. Hardy, preprint.